Sensors and Actuators B 176 (2013) 921–926

Contents lists available at SciVerse ScienceDirect

Sensors and Actuators B: Chemical

journal homepage: www.elsevier.com/locate/snb

Graphene paste electrode: Electrochemical behavior and analytical applications for the quantification of NADH

Aurélien Gasnier, M. Laura Pedano, María D. Rubianes*, Gustavo A. Rivas*

INFIQC, Departamento de Físico Química, Facultad de Ciencias Químicas, Universidad Nacional de Córdoba, Ciudad Universitaria, 5000 Córdoba, Argentina

ARTICLE INFO

Article history:
Received 18 July 2012
Received in revised form
19 September 2012
Accepted 26 September 2012
Available online 8 October 2012

Keywords:
Graphene
Graphene paste electrode
Composite electrode
Ascorbic acid
Dopamine
NADH

ABSTRACT

This work reports a critical study of the electrochemical behavior of a graphene paste electrode (GrPE) obtained by mixing graphite, mineral oil, and graphene obtained by reduction of graphene oxide with ascorbic acid and characterized by IR and Raman spectroscopy. The GrPE was characterized by scanning electron microscopy, cyclic voltammetry and amperometry. The effect of the GrPE composition on the electrochemical response of the resulting electrodes was studied using different redox probes. GrPE selectively catalyzes the electrooxidation of different bioanalytes such as ascorbic acid, dopamine and NADH without suffering common surface passivation. The advantages of GrPE for the simultaneous, selective and sensitive quantification of NADH in the presence of ascorbic acid are also reported.

1. Introduction

Graphene (Gr) is a two-dimensional sheet of sp^2-hybridized carbon atoms that form a flat hexagonal lattice [1,2]. Since the discovering by Geim et al. in 2004 [3], graphene has received enormous consideration due to its excellent electrical conductivity, mainly originated from the delocalized π bonds above and below the basal plane, its large surface area and low production costs [1,2]. Due to these excellent physical and chemical properties, Gr has become an interesting alternative for the development of electrical devices [4] and electrochemical sensors [1,2,5–8]. Graphene-based electrochemical sensors present a better performance compared to glassy carbon, graphite and even carbon nanotubes-based sensors, mainly due to sp^2-like planes and edge defects that are more exposed on the graphene nanosheets than on other carbon materials [2,9].

Different ways for synthesizing, modifying or suspending Gr for further electrode modification have been proposed [2,4]. Particularly interesting is the graphene paste electrode (GrPE), a composite electrode analogue to graphite paste electrode (CPE) [10] and carbon nanotubes paste electrode (CNTPE) [11,12], due to the advantages of the association of the excellent electrocatalytic activity of Gr with the unique properties of composite materials. The preparation of Gr-paste electrodes has been recently reported [13–16]. In fact, mixtures of graphene oxide (GrO) with mineral oil (approx. 76:24%, w/w, respectively) [14], graphite and hydrazine-reduced GrO with paraffin oil [15], and hydroquinone-reduced GrO with mineral oil [16] have been used for the amperometric detection of ascorbic acid (AA) [15], the voltammetric quantification of chlorpromazine [14], or as platform for further development of an immunosensor for hepatitis B [13] or a DNA sensor using daunomycin as redox probe [16].

The direct electrochemical quantification of nicotinamide adenine dinucleotide (NADH) has received considerable attention since it participates as coenzyme in many redox reactions catalyzed by dehydrogenases [17,18]. However, NADH direct oxidation is highly irreversible and the resulting products passivate the electrode [19–21]. Different strategies have been reported to solve this problem [22,23], most of them based on the use of carbon nanomaterials [2,19,22]. It is also well known that AA acts as an interferent in the electrochemical detection of NADH in biological samples [17,18,23]. Several strategies have been proposed to circumvent this problem [17,18,22,24,25]. A significant decrease in the overvoltage for NADH oxidation was observed using an ionic liquid/graphene/chitosan-modified electrode [26], and carbon nanosheets obtained by microwave plasma enhanced chemical vapor deposition with many graphene edges coatings [27]. Based on the excellent electrochemical activity of graphene toward NADH, an alcohol dehydrogenase/graphene-modified electrode was reported for the successful quantification of ethanol [28].

* Corresponding authors. Tel.: +54 351 4334169/80; fax: +54 351 4334188.
E-mail addresses: rubianes@fcq.unc.edu.ar (M.D. Rubianes), grivas@fcq.unc.edu.ar (G.A. Rivas).

0925-4005/$ – see front matter © 2012 Published by Elsevier B.V.
http://dx.doi.org/10.1016/j.snb.2012.09.092

This work reports the electrochemical behavior of a graphene paste electrode (GrPE) prepared by mixing different percentages of Gr (obtained by reducing GrO with AA) with graphite and mineral oil. The electrochemical behavior of the resulting GrPE was evaluated using different bioanalytes like AA, dopamine (Do), NADH and uric acid (UA) comparatively to that of the classical CPE. The application of the resulting GrPE for the sensitive quantification of AA and the sensitive and selective detection of NADH in the presence of AA without surface passivation was also assessed in this work. The synthesized GrO and Gr were characterized by FT-IR and Raman spectroscopy, while the resulting GrPE was characterized by field emission scanning electron microscopy (FE-SEM) as well as by electrochemical techniques (cyclic voltammetry (CV), differential pulse voltammetry (DPV) and amperometry).

2. Experimental

2.1. Apparatus and procedure

FT-IR spectra were obtained with a Nicolet FT-IR spectrometer (4.0 cm^{-1} resolution, 32 scans) by drop-coating and drying the samples dispersed in ethanol/water solution 1:1 on a ZnSe disk (Pike Technologies, 25 mm × 4 mm).

Raman spectra of GrO, Gr and graphite powders were obtained using a Horiba Jobin Yvon LabRam HR Raman spectrometer equipped with an Argon laser. Raman spectra were collected at 514.83 nm, using a pinhole of 100 μm and no attenuator filter, accumulating 20 spectra recorded for 10 s each.

Scanning electron microscopy (SEM) images were obtained with a field emission gun scanning electron microscope (FE-SEM, Zeiss, ∑IGMA model).

Electrochemical experiments were performed with an Autolab potentiostat (PGSTAT 101). A platinum wire and Ag/AgCl, 3 M KCl were used as counter and reference electrodes, respectively. All potentials are referred to the later. The electrodes were inserted into the cell through holes in its Teflon cover. Cyclic voltammetry experiments were performed at 0.100 V s^{-1}. The amperometric experiments were carried out by applying the desired potential and allowing the transient current to reach the steady-state value prior to the addition of the analyte and the subsequent current monitoring. A magnetic stirrer and a stirring bar provided the convective transport. DPV experimental conditions were the following: step potential: 0.01 V; modulation amplitude: 0.05 V; modulation time: 0.07 s; interval time: 0.2 s and scan rate 0.050 V s^{-1}.

2.2. Reagents

Graphite powder was purchased from Fisher (Chemical Scientific grade #38). Ascorbic acid (AA) and sodium phosphates were received from Baker; sulfuric acid and sodium hydroxide were purchased from Cicarelli; mineral oil was obtained from Aldrich; dopamine (Do) and nicotinamide adenine dinucleotide (NADH) were received from Sigma; and uric acid (UA) was purchased from Merck.

A 0.050 M phosphate buffer solution pH 7.40 was employed as supporting electrolyte. Ultrapure water (resistivity = 18 MΩ cm^{-1}) from a Millipore-MilliQ system was used for preparing all solutions. All the experiments were conducted at room temperature. All the reagents were used as received, without further purification.

2.3. Graphene oxide and graphene synthesis

GrO was synthesized from graphite using the Hummers method [4,29,30] and Gr was obtained by reduction of GrO with AA [31,32]. Briefly, graphite, sodium nitrate and potassium permanganate were added to concentrated sulfuric acid cooled to 0 °C. After heating at 35 °C for 30 min, the reaction mixture turned greenish and pasty, and when no more bubbling was observed, the reaction was carefully quenched by the slow addition of water with a pronounced temperature increase. The paste was kept at 90 °C for 15 min and turned brownish. After further dilution with water it was allowed to cool to 40 °C for 30 min, during which it turned yellow. Hydrogen peroxide was carefully added to form colorless soluble manganese sulfate. The resulting GrO was isolated while still warm by filtration and the yellow-brown filter cake was washed with warm 5% diluted hydrochloric acid and finally with water. The solid was solubilized in water by ultrasonication and any insoluble residue was removed by centrifugation. The resulting stable and brownish GrO aqueous solution was reduced by AA in a 1:1 Gr/AA mass ratio, at room temperature, overnight. The graphene black precipitate was filtrated, washed with water and dried at 100 °C for 8 h. The different steps of the synthesis were evaluated by FT-IR and Raman spectroscopy.

2.4. Preparation of graphene paste electrodes

Gr was manually grinded to a fine powder before preparation of the paste. Different Gr composites were obtained by mixing for 30 min in an agate mortar the desired amount of Gr, graphite, and mineral oil. The resulting composites were firmly packed into the cavity of a Teflon tube (3 mm diameter) to obtain the corresponding electrodes (GrPE). The electrical contact was established through a stainless steel screw. Prior to use, the GrPEs were repacked and polished on a weighing paper. Electrodes nomenclature according to the graphene/graphite/mineral oil ratio in (w/w) % are the following: CPE (0/70/30), Gr_{10}PE (10/50/40), Gr_{30}PE (30/30/40), Gr_{50}PE (50/0/50).

3. Results and discussion

3.1. Characterization of Gr and GrPE

3.1.1. Spectroscopic characterization of Gr

Fig. 1 displays the spectroscopic FT-IR (A) and Raman (B) characterization of graphite, GrO and Gr. The IR spectrum of graphene oxide (Fig. 1A, a) shows bands attributed to oxygen containing groups, which confirmed the successful oxidation of graphite. These bands are assigned to (O—H) stretching vibrations mode of intercalated water (3400 cm^{-1}); (C=O) stretching (1730 cm^{-1}); (CO epoxy) stretching (1225 cm^{-1}); and (CO alkoxy) stretching vibration (1050 cm^{-1}). The FT-IR spectrum of Gr (Fig. 1A, b) is similar to that of graphite (Fig. 1A, c) and agrees with those reported in the literature [33]. Strengthening and broadening of the signal at 1550 cm^{-1} denotes a degree of disorder and can be related to the bending of graphite sheets and the band at 1640 cm^{-1} can be assigned to skeletal vibrations of un-oxidized graphitic domains (C=C) [34]. Both spectra (Fig. 1A, b and c) differ from that of GrO (Fig. 1A, a) by the significant decrease of the bands at 3400, 1730 and 1050 cm^{-1}. Despite the small band at 1225 cm^{-1} in the Gr sample (Fig. 1A, b), its intensity significantly decreases and its position is shifted compared to the similar band in the GrO (Fig. 1A, a). These results confirm that most of the oxygenated functionalities have been removed and a substantial reduction of GrO to Gr has been achieved.

Fig. 1B shows Raman spectra for graphite powder (Fig. 1B, a), GrO flakes (Fig. 1B, b) and Gr powder (Fig. 1B, c). All Raman data show first and second-order spectra. The first-order spectrum of the pristine graphite powder (Fig. 1B, a) shows a characteristic strong G band at 1570 cm^{-1} and a weaker D band at 1340 cm^{-1}. The second-order spectrum of the starting graphite sample presents a

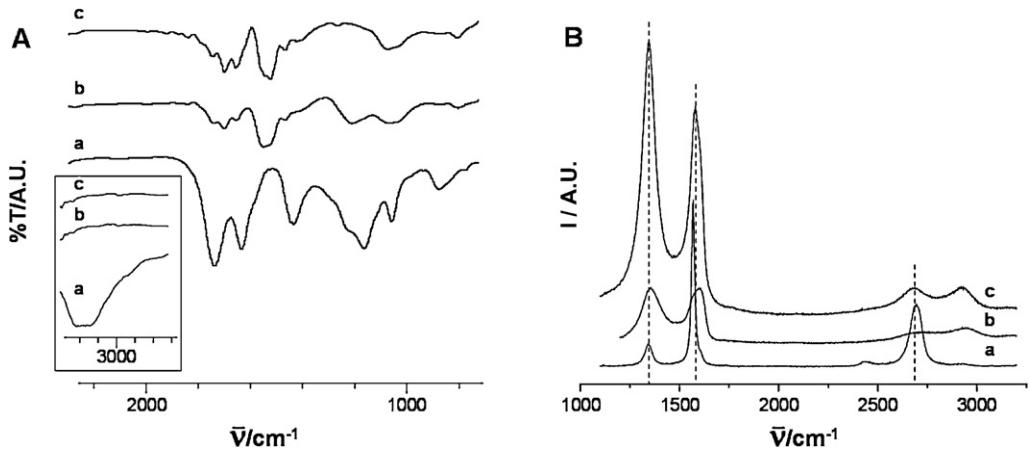

Fig. 1. (A) FT-IR spectra for graphene oxide (a), graphene (b) and graphite (c). (B) Raman spectra for graphite powder (a), graphene oxide (b) and graphene powder (c).

strong 2D band at 2690 cm^{-1} and a weak shoulder on the G band at 1608 cm^{-1} (D′ band). The spectrum of GrO (Fig. 1B, b) shows a dramatic increase in the ID/IG ratio compared to the starting graphite material (from 0.13 to 1.46), the 2D band is broader, the relative intensity is smaller compared to the G band, and an additional band appears at ~2920 cm^{-1} (D + D′ band). As it is known, the integrated intensity ratio of the D and G bands (ID/IG), as well as the relative intensity of the D′ band, increase with the amount of disorder in the graphitic layer. Thus, the observed features in the GrO spectra demonstrate that some structural disorder is produced in the GrO carbon lattice due to the oxidation process itself [35,36]. The Raman spectrum of the chemically reduced material Gr (Fig. 1B, c) exhibits an increment in the ID/IG ratio and the 2D and D + D′ bands become more intense and defined compared to the GrO sample (Fig. 1B, b). These results indicate that when the GrO sheet is deoxygenated by the chemical reduction process, the distortion of the 6-fold rings is removed and the carbon lattice returns to an essentially graphitic but highly defected state [35].

3.1.2. Scanning electron microscopy characterization of graphene composite

SEM characterization of different composites is presented in Fig. 2. The paste containing only graphite (A) shows conglomerations of flat graphite sheets domains over the whole surface. When the paste is only made of Gr (B), the structure looks more globular and compact, and the different regions are not completely fused one to each other. There is a higher amount of edge-plane borders which increases the roughness of this paste. In the case of a Gr/graphite mixture (C), combined but separated domains of almost rectangular flat graphite sheets with compact globular Gr grains can be observed. The Gr domains are not covered by graphite layers, leaving edge-planes exposed.

3.1.3. Macroscopic characteristics of graphene composites

At simple sight, the carbon paste looks light gray, uniform, and its consistence is soft, malleable, and rather humid. The $Gr_{50}P$ looks black, lumpy, and its consistence is hard, dry and more difficult to pack, polish and handle. The $Gr_{30}P$ looks light gray and its aspect and consistence is between the ones that correspond to carbon paste and $Gr_{50}P$. It is important to emphasize here that, as it was observed for the CNTPE [11], graphene paste is less malleable than its graphite counterpart and thus, it is necessary to adjust its oil content in order to get adequate mechanical characteristics.

3.1.4. Electrochemical characterization of graphene composites

The voltammetric behavior of CPE (dot) and $Gr_{30}PE$ (solid) in deoxygenated 0.050 M phosphate buffer solution pH 7.40 is illustrated in Fig. 3. The solvent oxidation at both electrodes starts at similar potentials (*ca.* 0.8 V), while at $Gr_{30}PE$ the reduction starts at potentials less negative than at CPE (*ca.* −0.2 V). Despite the potential window for $Gr_{30}PE$ is narrower compared to CPE, it is wide enough to allow for a good discrimination of anodic redox processes. Compared to CNTPE, the potential window is similar [11].

Fig. 4 shows the cyclic voltammetric profiles obtained at 0.100 V s^{-1} for 1.0×10^{-3} M AA (A), UA (B) and Do (C) at CPE, $Gr_{10}PE$, $Gr_{30}PE$ and $Gr_{50}PE$. As the Gr percentage in the composite increases, the overvoltage for AA oxidation decreases, the peaks are better defined and the associated currents increase. A decrease in the oxidation peak potential of 0.260 V is obtained for AA comparing CPE and $Gr_{50}PE$, clearly demonstrating that, even in the presence of the mineral oil, Gr retains an excellent electrochemical reactivity. It is important to remark that, compared to the previously reported GrPE [15], our GrPE allows to obtain a lower overvoltage for AA oxidation (0.250 V versus 0.110 V) and lower capacitive current. This different behavior could be associated with the different protocol for synthesizing Gr, the different

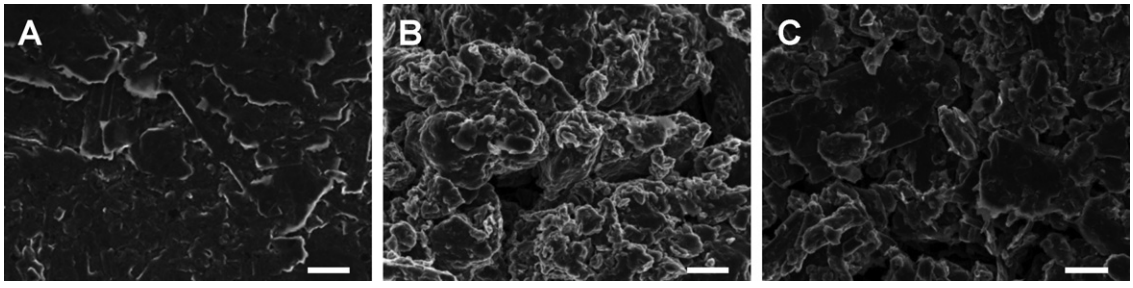

Fig. 2. SEM images for CPE (A), $Gr_{50}PE$ (B) and $Gr_{30}PE$ (C) at a 10.00K× magnification. Scale bar: 10 μm.

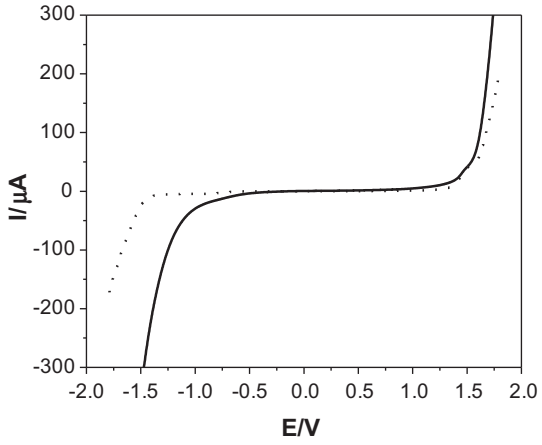

Fig. 3. Linear voltammograms obtained in deoxygenated 0.050 M phosphate buffer solution pH 7.40 at CPE (dot) and $Gr_{30}PE$ (solid). Scan rate: 0.100 V s^{-1}.

Table 1
Voltammetric parameters for the compounds shown in Fig. 4: AA, Do and UA, obtained at CPE, $Gr_{10}PE$, $Gr_{30}PE$ and $Gr_{50}PE$ obtained from the average of three repetitive measurements with different electrode surfaces each time.

Compound	Electrode	E_p [a]	ΔE_p [b]	$I_{p,ox}$ [c]
AA	CPE	0.40 ± 0.02		2.2 ± 0.1
	$Gr_{10}PE$	0.32 ± 0.03		1.56 ± 0.08
	$Gr_{30}PE$	0.170 ± 0.004		2.29 ± 0.07
	$Gr_{50}PE$	0.139 ± 0.005		2.37 ± 0.05
Do	CPE	0.28 ± 0.03	0.21 ± 0.04	2.7 ± 0.1
	$Gr_{10}PE$	0.210 ± 0.005	0.132 ± 0.007	2.83 ± 0.03
	$Gr_{30}PE$	0.179 ± 0.003	0.088 ± 0.004	3.3 ± 0.1
	$Gr_{50}PE$	0.183 ± 0.002	0.084 ± 0.002	3.6 ± 0.3
UA	CPE	0.42 ± 0.02		2.2 ± 0.1
	$Gr_{10}PE$	0.333 ± 0.005		3.4 ± 0.6
	$Gr_{30}PE$	0.326 ± 0.001		4.1 ± 0.2
	$Gr_{50}PE$	0.329 ± 0.002		4.2 ± 0.5

[a] Oxidation potential in (V).
[b] Peak potential separation in (V).
[c] Oxidation peak current in (A, $\times 10^{-5}$).

Gr content in the paste and the previous grinding of Gr introduced in the current work, which could allow for a better inter-particle connection.

For UA (Fig. 4B), at Gr-based composites, there is an important decrease in the oxidation overpotential and a significant enhancement in the oxidation peak current (almost 100%) compared to CPE. However, at variance with the behavior observed for AA, the variation of the Gr amount in the paste does not produce a significant change in the voltammetric behavior. Regarding the electrochemical response of Do (Fig. 4C), the oxidation potential and the peak potential separation (ΔE_p) decrease as the amount of Gr in the paste increases, indicating an improvement in the reversibility of the electrooxidation process. The voltammetric parameters for AA, UA, and Do electrooxidation obtained at the different electrodes are summarized in Table 1 and are comparable to other graphene-based electrodes [2,37,38]. The electrochemical behavior for UA at GrPE is similar to that observed at CNTPE, whereas for Do and AA, the response at GrPE is even better [15].

It is worth to note that increasing the Gr content beyond 30% (w/w) the electrocatalytic response of the electrode does not improve significantly. Additionally, the paste containing 50% Gr is harder to polish and more difficult to handle than the others, and presents higher capacitive currents. Therefore, the $Gr_{30}PE$ represents the best compromise between high electrochemical activity, minimal capacitive currents, high reproducibility and better malleability. With this electrode, a good electrocatalytic activity can be obtained with a material much cheaper and easier to synthesize than CNTs and without the risk of metallic contamination.

3.2. Analytical applications of GrPE

The suitability of $Gr_{30}PE$ for developing sensitive electrochemical sensors for AA and for the quantification of NADH in the presence of AA was also evaluated. Fig. 5A depicts the amperometric response obtained at 0.125 V at CPE (a) and $Gr_{30}PE$ (b) for successive additions of 1.0×10^{-5} M AA. In agreement with the results obtained by CV (Fig. 4A), almost no signal is observed at this potential at CPE (a), while a fast response is attained at $Gr_{30}PE$ (b). The sensitivity at $Gr_{30}PE$ was (20 ± 2) μA/mM obtained with three different electrode surfaces using the same paste; while the detection limit was 0.3 μM, taken as ($3 \times \sigma/S$) (where S is the sensitivity and σ is the standard deviation of the blank signal). Therefore, both analytical parameters largely improved compared to CPE ((0.32 ± 0.02) μA/mM and 9 μM, respectively). Even when the sensitivity reported here is smaller and the detection limit is higher than those reported by Li et al. [15] (33.3 μA/mM and 7.0×10^{-8} M, respectively), it is important to remark that the determination of AA in the present work is performed at working potentials 0.185 V smaller, enabling the determination of AA at potentials where the interference of common electroactive compounds can be avoided.

Fig. 5B compares the amperometric response at 0.470 V for 1.0×10^{-5} M NADH obtained at CPE (a) and at $Gr_{30}PE$ (b). After 20 min of continuous operation, the signal decreases by 53% at CPE, while at $Gr_{30}PE$ the amperometric response remains at 91% of the initial current. These results prove that there is a very limited passivation by NADH oxidation products and demonstrate that $Gr_{30}PE$ is a robust, stable, and reproducible platform, suitable for

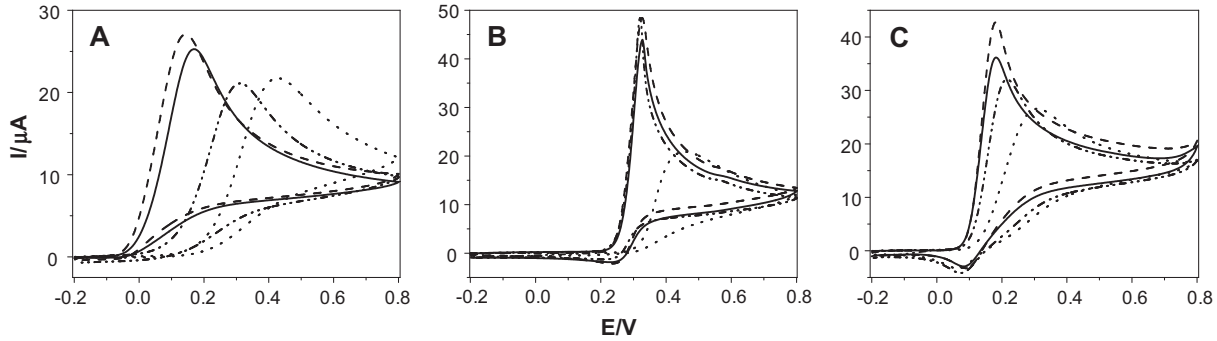

Fig. 4. Voltammetric profiles obtained at 0.100 V s^{-1} for 1.0×10^{-3} M AA (A), UA (B), and Do (C) at CPE (dot), $Gr_{10}PE$ (dash-dot), $Gr_{30}PE$ (solid) and $Gr_{50}PE$ (dash). Other conditions as in Fig. 3.

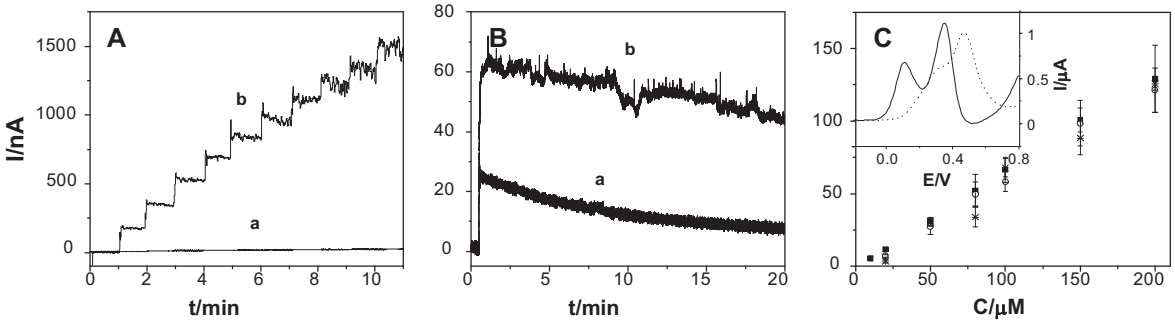

Fig. 5. (A) Amperometric recordings at 0.125 V obtained at CPE (a) and Gr_{30}PE (b) for successive additions of 1.0×10^{-5} M AA. (B) Amperometric response for 1.0×10^{-5} M NADH at 0.470 V obtained at CPE (a) and at Gr_{30}PE (b). (C) Calibration plots obtained at Gr_{30}PE for NADH in the absence (full squares) and in the presence of 1.0×10^{-5} M (circles) and 5.0×10^{-5} M (stars) AA. Inset: DPVs for 5.0×10^{-5} M AA and 1.5×10^{-4} M NADH obtained at CPE (dot) and Gr_{30}PE (solid). Other conditions as in Fig. 3.

continuous monitoring of NADH. Since at Gr_{30}PE NADH and AA are oxidized at very different peak potentials (0.47 and 0.17 V, respectively), the possibility to quantify NADH in presence of AA at Gr_{30}PE was evaluated. Fig. 5C (inset) shows DPVs for 5.0×10^{-5} M AA and 1.5×10^{-4} M NADH obtained at CPE (dot) and Gr_{30}PE (solid). At CPE, the contributions from NADH and AA oxidation cannot be distinguished because the oxidation overvoltages for both compounds are similar. On the contrary, at Gr_{30}PE, the two processes are separated due to the preferential catalytic oxidation of AA on this surface. Fig. 5C displays calibration plots obtained at Gr_{30}PE for NADH in the absence (full squares) and in the presence of 1.0×10^{-5} M (circles) and 5.0×10^{-5} M (stars) AA. The sensitivities obtained from the average of three calibration plots, performed with three different electrode surfaces using the same paste, were (6.7 ± 0.5), (6.6 ± 0.5), and (6.9 ± 0.2) μA/mM in the absence and in the presence of 1.0×10^{-5} M and 5.0×10^{-5} M AA, respectively. These results indicate that the presence of AA does not modify the sensitivity of Gr_{30}PE toward NADH, and demonstrate that Gr_{30}PE itself exhibits good selectivity, great versatility and potential analytical applications in a variety of systems.

4. Conclusions

The proposed graphene paste electrode obtained by mixing graphene obtained from AA-reduced GrO, graphite and mineral oil presents an excellent electrochemical response, better than that of its analogue CPE and comparable or even better than that of CNTPE. Moreover, GrPE is considerably less expensive and easier to prepare than CNTPE, and does not present the risk for contamination with metal catalyst. Compared to the recently reported graphene paste electrodes, the GrPE proposed here presents clear advantages: is very reproducible, is more electroactive (clearly demonstrated using different redox probes), presents smaller capacitive currents and is resistant to passivation. In this way, it was possible to accomplish the successful quantification of NADH in the presence of AA without fouling of the surface. Compared to other Gr-based electrochemical sensors, the GrPE proposed here presents the great advantage of the successful association of the excellent electrocatalytic properties of Gr and the unique properties of composite materials connected to their robustness, the feasibility to incorporate biomolecules, catalysts, mediators and stabilizers, and the easiness and short time for preparation. Therefore, considering the versatility of composite materials and the clear advantages of this electrode material, it is expected that GrPE receives great attention and opens a completely new scenario in the field of Gr-based electrochemical (bio)sensors.

Acknowledgements

Authors thank CONICET, SECyT-UNC, ANPCyT, Ministry of Science and Technology of Cordoba for the financial support. AG acknowledges SECyT-UNC for the postdoctoral fellowship.

References

[1] Y. Shao, J. Wang, H. Wu, J. Liu, I.A. Aksay, Y. Lin, Graphene based electrochemical sensors and biosensors: a review, Electroanalysis 22 (10) (2010) 1027–1036.
[2] K.R. Ratinac, W. Yang, J.J. Gooding, P. Thordarson, F. Braet, Graphene and related materials in electrochemical sensing, Electroanalysis 23 (2011) 803–826.
[3] K.S. Novoselov, A.K. Geim, S.V. Morozov, D. Jiang, Y. Zhang, S.V. Dubonos, I.V. Grigorieva, A.A. Firsov, Electric field effect in atomically thin carbon films, Science 306 (2004) 666–669.
[4] S. Park, R.S. Ruoff, Chemical methods for the production of graphenes, Nature Nanotechnology 4 (2009) 217–224.
[5] W. Yang, K.R. Ratinac, S.P. Ringer, P. Thordarson, J.J. Gooding, F. Braet, Carbon nanomaterials in biosensors: should you use nanotubes or graphene? Angewandte Chemie International Edition 49 (2010) 2114–2138.
[6] C. Shan, H. Yang, J. Song, D. Han, A. Ivaska, L. Niu, Direct electrochemistry of glucose oxidase and biosensing for glucose based on graphene, Analytical Chemistry 81 (2009) 2378–2382.
[7] T. Kuila, S. Bose, P. Khanra, A.K. Mishra, N.H. Kim, J.H. Lee, Recent advances in graphene-based biosensors, Biosensors and Bioelectronics 26 (2011) 4637–4648.
[8] Y. Liu, X. Dong, P. Chen, Biological and chemical sensors based on graphene materials, Chemical Society Reviews 41 (2012) 2283–2307.
[9] F. Banhart, J. Kotakoski, A.V. Krasheninnikov, Structural defects in graphene, ACS Nano 5 (2011) 26–41.
[10] I. Svancara, K. Vytras, K. Kalcher, A. Walcarius, J. Wang, Carbon paste electrodes in facts, numbers, and notes: a review on the occasion of the 50-years jubilee of carbon paste in electrochemistry and electroanalysis, Electroanalysis 21 (2009) 7–28.
[11] M.D. Rubianes, G.A. Rivas, Carbon nanotubes paste electrode, Electrochemistry Communications 5 (2003) 689–694.
[12] G.A. Rivas, M.D. Rubianes, M.L. Pedano, N.F. Ferreyra, G.L. Luque, M.C. Rodriguez, S.A. Miscoria, Carbon nanotubes paste electrodes. A new alternative for the development of electrochemical sensors, Electroanalysis 19 (2007) 823–831.
[13] K.-J. Huang, J. Li, Y.-M. Liu, X. Cao, S. Yu, M. Yu, Disposable immunoassay for hepatitis B surface antigen based on a graphene paste electrode functionalized with gold nanoparticles and a Nafion-cysteine conjugate, Microchimica Acta 177 (2012) 419–426.
[14] M.H. Parvin, Graphene paste electrode for detection of chlorpromazine, Electrochemistry Communications 13 (2011) 366–369.
[15] F. Li, J. Li, Y. Feng, L. Yang, Z. Du, Electrochemical behavior of graphene doped carbon paste electrode and its application for sensitive determination of ascorbic acid, Sensors and Actuators B 157 (2011) 110–114.
[16] Y. Bo, W. Wang, J. Qi, S. Huang, A DNA biosensor based on graphene paste electrode modified with Prussian blue and chitosan, Analyst 136 (2011) 1946–1951.
[17] A.L. Lehninger, D.L. Nelson, M.M. Cox, Lehninger Principles of Biochemistry, fifth ed., W.H. Freeman, New York, 2008.
[18] A. Radoi, D. Compagnone, Recent advances in NADH electrochemical sensing design, Bioelectrochemistry 76 (2009) 126–134.
[19] H. Jaegfeldt, Adsorption and electrochemical oxidation behaviour of NADH at a clean platinum electrode, Journal of Electroanalytical Chemistry 110 (1980) 295–302.
[20] J. Moiroux, P.J. Elving, Effects of adsorption, electrode material, and operational variables on the oxidation of dihydronicotinamide adenine dinucleotide at carbon electrodes, Analytical Chemistry 50 (1978) 1056–1062.

[21] M.A. Hayes, W.G. Kuhr, Preservation of NADH voltammetry for enzyme-modified electrodes based on dehydrogenase, Analytical Chemistry 71 (1999) 1720–1727.
[22] C.E. Banks, R.G. Compton, Exploring the electrocatalytic sites of carbon nanotubes for NADH detection: an edge plane pyrolytic graphite electrode study, Analyst 130 (2005) 1232–1239.
[23] J. Chen, J.C. Bao, C.X. Cai, T.H. Lu, Electrocatalytic oxidation of NADH at an ordered carbon nanotubes modified glassy carbon electrode, Analytica Chimica Acta 516 (2004) 29–34.
[24] J. Ping, Y. Wang, K. Fan, J. Wu, Y. Ying, Direct electrochemical reduction of graphene oxide on ionic liquid doped screen-printed electrode and its electrochemical biosensing application, Biosensors and Bioelectronics 28 (2011) 204–209.
[25] C. Shan, H. Yang, D. Han, Q. Zhang, A. Ivaska, L. Niu, Electrochemical determination of NADH and ethanol based on ionic liquid-functionalized graphene, Biosensors and Bioelectronics 25 (2010) 1504–1508.
[26] Ch. Shan, H. Yang, D. Han, Q. Zhang, A. Ivaska, L. Niu, Electrochemical determination of NADH and ethanol based on ionic liquid-functionalized graphene, Biosensors and Bioelectronics 25 (2010) 1504–1508.
[27] Z. Wang, M. Shoji, H. Ogata, Electrochemical determination of NADH based on MPECVD carbon nanosheets, Talanta 99 (2012) 487–491.
[28] K. Guo, K. Qian, S. Zhang, J. Kong, Ch. Yu, B. Liu, Bio-electrocatalysis of NADH and ethanol based on graphene sheets modified electrodes, Talanta 85 (2011) 1174–1179.
[29] W.S. Hummers, R.E. Offeman, Preparation of graphitic oxide, Journal of the American Chemical Society 80 (1958) 1339.
[30] D.R. Dreyer, S. Park, C.W. Bielawski, R.S. Ruoff, The chemistry of graphene oxide, Chemical Society Reviews 39 (2010) 228–240.
[31] J. Zhang, H. Yang, G. Shen, P. Cheng, J. Zhang, S. Guo, Reduction of graphene oxide via L-ascorbic acid, Chemical Communications 46 (2010) 1112–1114.
[32] V. Dua, S.P. Surwade, S. Ammu, S.R. Agnihotra, S. Jain, K.E. Roberts, S. Park, R.S. Ruoff, S.K. Manohar, All-organic vapor sensor using inkjet-printed reduced graphene oxide, Angewandte Chemie International Edition 49 (2012) 1–5.
[33] J.I. Paredes, S. Villar-Rodil, A. Martínez-Alonso, J.M.D. Tascón, Graphene oxide dispersions in organic solvents, Langmuir 24 (2008) 10560–10564.
[34] J. Shen, N. Li, M. Shi, Y. Hu, M. Ye, Covalent synthesis of organophilic chemically functionalized graphene sheets, Journal of Colloid and Interface Science 348 (2010) 377–383.
[35] J.I. Paredes, S. Villar-Rodil, P. Solís-Fernandez, A. Martínez-Alonso, J.M.D. Tascón, Atomic force and scanning tunneling microscopy imaging of graphene nanosheets derived from graphite oxide, Langmuir 25 (2009) 5957–5968.
[36] Y. Zhu, S. Murali, W. Cai, X. Li, J.W. Suk, J.R. Potts, R.S. Ruoff, Graphene and graphene oxide: synthesis, properties and applications, Advanced Materials 22 (2010) 3906–3924.
[37] Z.-H. Sheng, X.-Q. Zheng, J.-Y. Xu, W.-J. Bao, F.B. Wang, X.-H. Xia, Electrochemical sensor based on nitrogen doped graphene: simultaneous determination of ascorbic acid, dopamine and uric acid, Biosensors and Bioelectronics 34 (2012) 125–131.
[38] J. Wang, S. Yang, D. Guo, P. Yu, D. Li, J. Ye, L. Mao, Comparative studies on electrochemical activity of graphene nanosheets and carbon nanotubes, Electrochemistry Communications 11 (2009) 1892–1895.

Biographies

Aurelien Gasnier received his M.S. in organic synthesis in 2005 from Université Paris-Sud (France). During his Ph.D. at Université Joseph Fourier (France) he focused on electroactive terpyridine-cyclam coordination polymers under the co-direction of Profs. Moutet, Royal and Térech. After one year at University of Chicago (U.S.) in the group of Prof. Luping Yu, he joined the group of Prof. Gustavo Rivas at Universidad Nacional de Córdoba (Argentina) in 2010 and is now dedicated to the development of modified carbon electrodes.

María L. Pedano obtained her PhD in Chemistry (2006) from Córdoba National University (Argentina) and was awarded the Prize Enrique Herrero Ducloux, from the Argentinean Chemical Association, to the best Ph.D. thesis in Physical Chemistry. She performed postdoctoral research at Joseph Fourier University (France) and at Northwestern University (U.S.A.). At present, Dr. Pedano is assistant professor at the Department of Physical Chemistry (Faculty of Chemical Sciences, Córdoba National University), an active member of the Biosensor's Group, and Adjunt Researcher at CONICET. Her research focuses on plasmonic nanostructures and its application to Raman spectroscopy and electrochemical biosensors.

María D. Rubianes obtained her Ph.D. in Chemistry (2005) from the Córdoba National University (Argentina). She did the postdoctoral training in the group of Polymers at the Organic Chemistry Department, Faculty of Chemical Sciences (Cordoba National University). At present, she is assistant professor at the Department of Physical Chemistry, Faculty of Chemical Sciences of Cordoba National University and Adjunt Researcher at CONICET. Dr. Rubianes is an active member of the Biosensors Group at the Physical Chemistry Department, and her research interests focus on the development and characterization of electrochemical (bio)sensors based on the use of nanostructured materials and modified polymers.

Gustavo A. Rivas obtained his PhD in Chemistry (1991) from the National University of Córdoba (Argentina). Between 1994 and 1996 he did the postdoctoral training at the University of Valence (Spain) and New Mexico State University, Las Cruces (USA). At present, he is full professor at the National University of Córdoba and Principal Researcher at CONICET. Professor Rivas has received the Ranwell Caputto (2001) and Rafael Labriola (2004) Award. His research focused on the development and characterization of electrochemical enzymatic and affinity (bio)sensors based on the use of nanomaterials, polymers and biomolecules.